DMRS Design and Channel Estimation for LTE-Advanced MIMO Uplink

Xiaolin Hou, Zhan Zhang, Hidetoshi Kayama
DOCOMO Beijing Communications Laboratories Co., Ltd.
Beijing, China
Email: {hou, z.zhan, kayama}@docomolabs-beijing.com.cn

***Abstract*—In 3GPP long term evolution (LTE) uplink, single transmit antenna is adopted due to its simplicity and acceptable performance. However, in order to satisfy the higher requirement of LTE-Advanced (LTE-A) on uplink spectrum efficiency, multiple transmit antennas must be supported in LTE-A uplink. At the same time, the backwards compatibility to LTE should be taken into considerations. Therefore, the demodulation reference signal (DMRS) as well as channel estimation have to be re-designed for LTE-A uplink to support multiple-input multiple-output (MIMO) transmission. In this paper, we propose the DMRS design for LTE-A MIMO uplink via frequency domain code division multiplexing (FD-CDM) with the maximum distance binding (MDB), which can minimize the interference among multiple transmit antennas. More importantly, it is backwards compatible to the DMRS in LTE uplink, i.e., few modifications to the current specifications are needed. Furthermore, the improved uplink channel estimation with dynamic channel impulse response reservation (DCIR^2) and frequency domain windowing/dewindowing is proposed to enhance the channel estimation accuracy and uplink reliability for both LTE and LTE-A. Computer simulations demonstrate their effectiveness.**

I. Introduction

Considering the cost of user equipment (UE), the specification schedule and the fact that the 3GPP long term evolution (LTE) uplink with single transmit antenna can already satisfy the uplink peak spectrum efficiency requirement defined in [1], in the 3GPP TSG RAN WG1 meeting #47bis it was decided that uplink multiple-input multiple-output (MIMO) will not be supported in the first release of LTE (rel-8) [2]. Recently, 3GPP has started the study item (SI) on LTE-Advanced (LTE-A) and the requirements of LTE-A are quit ambitious [3], especially for the uplink, e.g. the uplink peak spectrum efficiency should reach 15bps/Hz, which can not be achieved by the LTE uplink with single transmit antenna [4]. Therefore, MIMO including transmit diversity (TxD), single-user MIMO (SU-MIMO) and multiple-user MIMO (MU-MIMO) should be incorporated into the uplink of LTE-A [5-7]. Furthermore, LTE-A must have the backwards compatibility to LTE [3].

LTE uplink is based on single-carrier frequency division multiple access (SC-FDMA) due to its low peak-to-average power ratio (PAPR). There are two types of reference signal in LTE uplink: demodulation reference signal (DMRS) and sounding reference signal (SRS) [4]. Both DMRS and SRS need to be enhanced or revised to support the uplink MIMO transmission in LTE-A and in this study we only focus on DMRS design and related channel estimation for the physical uplink shared channel (PUSCH).

As for the DMRS design to support uplink MIMO, there are two possible ways forward, i.e., time-domain code division multiplexing (TD-CDM) [8-11] and frequency-domain code division multiplexing (FD-CDM) [10-13]. TD-CDM has several apparent disadvantages, such as can only support two transmit antennas, is only valid for low mobility cases and cannot support PUSCH hopping within one subframe. Therefore, FD-CDM is a natural and better choice. However, there are still two remaining problems to be solved, i.e., how to assign different DMRS sequences to different transmit antennas and how to ensure the backwards compatibility to LTE. On the other hand, channel estimation for LTE uplink is generally based on discrete Fourier transform (DFT) with cyclic prefix reservation (CPR) [14]. Because this method does not consider the channel impulse response (CIR) energy leakage problem and the frequency domain Gibbs phenomenon in engineering practice, the channel estimation accuracy as well as uplink reliability will deteriorate significantly, especially when the number of resource blocks (RB) allocated to a given UE is not so large.

In this paper, we propose the DMRS design based on FD-CDM with the maximum distance binding (MDB) for LTE-A MIMO uplink, which can minimize the interference among multiple transmit antennas and meanwhile is backwards compatible to LTE. Furthermore, an improved uplink channel estimation method with dynamic channel impulse response reservation (DCIR^2) and frequency domain windowing/dewindowing is proposed, where the CIR energy leakage problem and the frequency domain Gibbs phenomenon will be properly handled according to the dynamic uplink RB allocation for different UEs. Therefore, the channel estimation accuracy and uplink reliability will be effectively improved.

The rest of this paper is organized as follows: Section II briefly introduces the DMRS structure and channel estimation in current LTE uplink. In Section III we propose the DMRS design and improved channel estimation for LTE-A MIMO uplink. Section IV provides computer simulations and conclusions can be found in Section V.

II. DMRS Structure and Channel Estimation for LTE Uplink

In LTE uplink, the DMRS for PUSCH in the frequency domain will be mapped to the same set of physical resource

978-1-4244-2515-0/09/$25.00 ©2009 IEEE

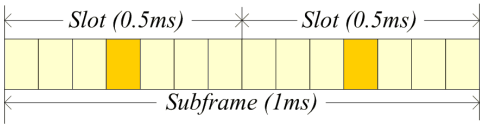

Fig. 1. DMRS in LTE uplink.

blocks (PRB) used for the corresponding PUSCH transmission with the same length expressed by the number of subcarriers, while in the time domain DMRS will occupy the $4th$ SC-FDMA symbol in each slot for frame structure type 1 with normal cyclic prefix (CP), as shown in Fig. 1.

In order to support a large number of UEs in multiple cells, a large number of different DMRS sequences are needed. A DMRS sequence $r_{u,v}^{(\alpha)}(n)$ is defined by a cyclic shift (CS) α of a base sequence $\bar{r}_{u,v}(n)$ according to

$$r_{u,v}^{(\alpha)}(n) = e^{j\alpha n}\bar{r}_{u,v}(n), 0 \leq n < M_{sc}^{RS} \tag{1}$$

where $M_{sc}^{RS} = mN_{sc}^{RB}$ is the length of DMRS sequence, m is the RB number and N_{sc}^{RB} is the subcarrier number within each RB. Multiple DMRS sequences can be derived from a single base sequence through different values of α.

The definition of the base sequence depends on the sequence length. For $M_{sc}^{RS} \geq 3N_{sc}^{RB}$, the base sequence is defined as the cyclic extension of the Zadoff-Chu sequence [15]

$$\bar{r}_{u,v}(n) = x_q(n \bmod N_{ZC}^{RS}), 0 \leq n < M_{sc}^{RS} \tag{2}$$

where $x_q(m), 0 \leq m < N_{ZC}^{RS} - 1$ is the q_{th} root Zadoff-Chu sequence and N_{ZC}^{RS} is the length of Zadoff-Chu sequence that is given by the largest prime number such that $N_{ZC}^{RS} < M_{sc}^{RS}$. For $M_{sc}^{RS} < 3N_{sc}^{RB}$, the base sequence is defined as the computer generated constant amplitude zero autocorrelation (CG-CAZAC) sequence

$$\bar{r}_{u,v}(n) = e^{j\varphi(n)\pi/4}, 0 \leq n < M_{sc}^{RS} \tag{3}$$

where the values of $\varphi(n)$ are given in [4].

Base sequences $\bar{r}_{u,v}(n)$ are divided into 30 groups with $u \in 0, 1, ..., 29$. Each group contains one base sequence $(v = 0)$ with $1 \leq m \leq 5$ and two base sequences $(v = 0, 1)$ with $6 \leq m \leq N_{RB}^{max,UL}$, where $N_{RB}^{max,UL}$ is the maximum RB number in the uplink. In order to reduce inter-cell interference (ICI), neighboring cells should select DMRS sequences from different base sequence groups. Furthermore, there are 3 kinds of hopping defined for the DMRS in LTE uplink, i.e., group hopping, sequence hopping and CS hopping, where CS hopping should always be enabled in each slot.

The CS value α in a slot is given by $\alpha = 2\pi n_{cs}/12$ with

$$n_{cs} = (n_{DMRS}^{(1)} + n_{DMRS}^{(2)} + n_{PRS})/12 \tag{4}$$

where $n_{DMRS}^{(1)}$ is a broadcast value, $n_{DMRS}^{(2)}$ is included in the uplink scheduling assignment and n_{PRS} is given by a cell-specific pseudo-random sequence.

Channel estimation for LTE uplink can be based on DFT with CPR [14]. Because the RB allocation for a given UE is generally only a small portion of the overall uplink bandwidth, the CIR energy leakage as shown in Fig. 2 will be observed in practice. In Fig. 2, the first and the second rows are for 2×2 and 4×4 MIMO cases, while the left and the right columns are for RB# = 1 and RB# = 10 cases, respectively. It's obvious that the smaller the RB number, the more severe the CIR energy leakage. Furthermore, the frequency domain Gibbs phenomenon will appear at the edge of assigned consecutive RBs for a given UE due to the signal discontinuities. Therefore, the channel estimation accuracy as well as uplink reliability will deteriorate significantly in engineering practice.

III. DMRS Design and Improved Channel Estimation for LTE-A MIMO Uplink

In order to support MIMO transmission in LTE-A uplink, the DMRS design with backwards compatibility and the improved channel estimation will be proposed in this section.

A. DMRS Design

For UE with $n_T \geq 2$ transmit antennas, FD-CDM will be adopted to separate the multiple transmit antennas, with the following restriction satisfied.

$$n_{cs,i} = (n_{cs,0} + \frac{C}{n_T} \cdot i) \bmod (C), i = 0, 1, ..., n_T - 1 \tag{5}$$

where $n_{cs,i}$ corresponds to the CS value of DMRS for the ith transmit antenna and C is the constant value 12 for PUSCH. The CS value of DMRS for the first transmit antenna $\alpha_0 = 2\pi n_{cs,0}/12$ is exactly the same as that for the single transmit antenna case in LTE. Therefore, all the original CS hopping designs for the single transmit antenna UE in LTE can be kept

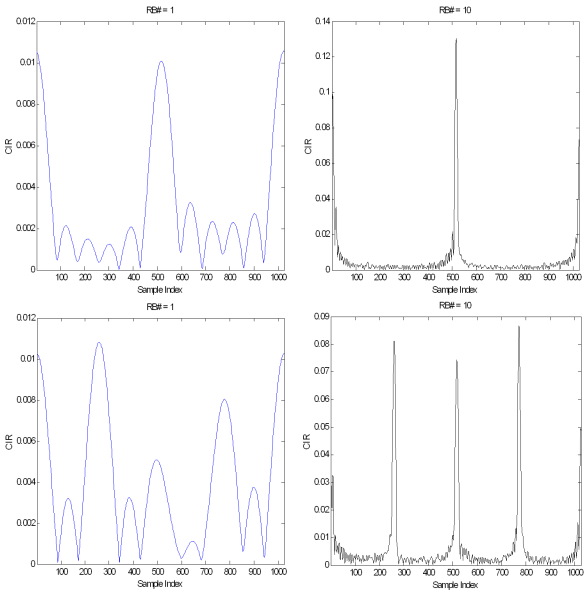

Fig. 2. CIR energy leakage.

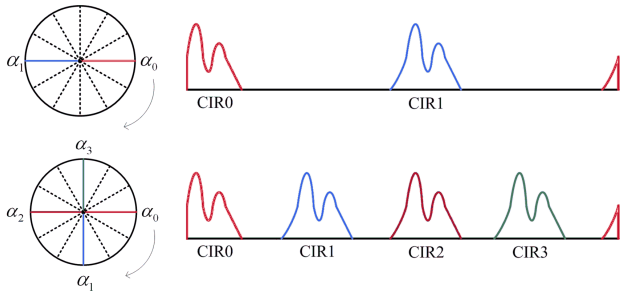

Fig. 3. DMRS design with MDB.

unchanged for the multiple transmit antennas UE in LTE-A, once the constraint in (5) is satisfied.

Because this DMRS design can be viewed as binding together the CS values of DMRS as well as the CIR positions of different transmit antennas with the maximum distance constraint, as illustrated in Fig. 3 (Note that the relationship between α_i and α_0 will keep unchanged during CS hopping), we simply call it DMRS design with the maximum distance binding (MDB). Its benefits include: First, the distance between CIRs of different transmit antennas in the time domain can be always maximized, therefore, the interference between DMRS of different transmit antennas can be minimized; Second, no additional signaling is required for CS hopping to support uplink MIMO transmission, therefore, it is backwards compatible to LTE; Third, it provides the unified operation for different transmit antenna number cases.

Actually, the same DMRS design principle can also be applied to the uplink MU-MIMO transmission with single transmit antenna UEs. Now it only requires some constraint in the uplink scheduling assignment for the CS of DMRS (because $n^{(1)}_{DMRS}$ and n_{PRS} are the same for all the UEs in the same cell, respectively) as follows

$$n^{(2)}_{DMRS,i} = (n^{(2)}_{DMRS,0} + \frac{C}{n_T} \cdot i) \text{mod}(C), i = 0, 1, ..., n_T - 1 \quad (6)$$

where $n^{(2)}_{DMRS,0}$ is the scheduled value for the first UE and n_T now represents the UE number.

In order to support the above CS scheduling constraint for MU-MIMO transmission, we have two possible options:

- Option 1: No signaling modification
  Because the current LTE specification only supports 8 possible values for $n^{(2)}_{DMRS}$, a limited number of combinations can be chosen in the uplink scheduling with the MDB constraint (6) satisfied. Therefore, for the 2-user case, $n^{(2)}_{DMRS,i} \in \{(0,6),(2,8),(3,9),(4,10)\}$; while for the 4-user case, $n^{(2)}_{DMRS,i} \in \{(0,3,6,9)\}$.
- Option 2: Slight signaling modification
  If the specific field in downlink control information (DCI) format 0 for the CS of DMRS can be increased from 3 bits to 4 bits, all the possible combinations in the CS scheduling for MU-MIMO transmission can be supported with the MDB constraint (6) satisfied.

B. Improved Channel Estimation

The improved uplink channel estimation at each receive antenna of eNB is shown in Fig. 4, taking user 1 for example. After serial-to-parallel (S/P) conversion and K-point fast Fourier transform (FFT), the received signal is transformed into the frequency domain. Because each UE (excluding UEs in the same MU-MIMO transmission) occupies different RBs in the uplink, we can first separate different UEs by way of frequency division multiplexing (FDM). Then multiply the separated received signal by the complex conjugate of the DMRS sequence assigned for the $1st$ transmit antenna and perform K-point inverse FFT (IFFT) to get the superposed CIRs in the time domain. After the operation of DCIR^2 that will be explained in more details later, we can separate the CIRs for different transmit antennas (for SU-MIMO case) or different users (for MU-MIMO case) by way of CDM. Finally, the complete channel estimation result can be obtained by K-point FFT and provided to the MIMO detection block. Furthermore, in order to suppress the frequency domain Gibbs phenomenon at the edge of assigned consecutive RBs for a given UE in channel estimation, UE-specific frequency-domain windowing/dewindowing blocks can be further added to improve channel estimation accuracy with some additional complexity. Note that the proposed improved uplink channel estimation can be applied to not only LTE-A MIMO uplink, but also LTE single-input single-output (SISO) or single-input multiple-output (SIMO) uplink.

As for the operation of DCIR^2, the dynamically reserved CIR for each transmit antenna consists of 2 parts with respect to the timing positions, i.e., $(\frac{C}{n_T} \cdot i) \cdot K, i = 0, 1, ..., n_T - 1$:

- Right part
  There are $\lambda \cdot CP$ samples preserved with the following right boundary

$$(\frac{C}{n_T} \cdot i) \cdot K + \lambda \cdot CP - 1, i = 0, 1, ..., n_T - 1 \quad (7)$$

  where CP is the cyclic prefix length of the SC-FDMA symbol and λ is an adjustable parameter ($0 \leq \lambda < 1$) that can be optimized in practical implementations.
- Left part
  There are $\mu \cdot \Delta$ samples preserved with the following left boundary

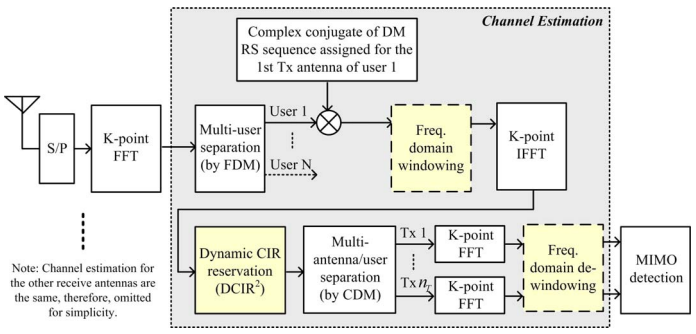

Fig. 4. The improved uplink channel estimation.

$$[(\frac{C}{n_T}\cdot i)\cdot K-\mu\cdot\Delta+K]\text{mod}(K), i=0,1,...,n_T-1 \quad (8)$$

where Δ is the main lobe width of CIR energy leakage ($\Delta = \frac{K}{12\cdot RB\#}$) and μ is an adjustable parameter ($0 \leq \mu < \frac{K/n_T - CP}{\Delta}$) that can be optimized in practical implementations. In order to simplify the adjustment, we can define $\tilde{\Delta} = \frac{K}{12}$ and $\tilde{\mu} = \frac{\mu}{RB\#}$, therefore, $\tilde{\Delta}$ becomes a constant and only $\tilde{\mu}$ should be adjusted.

The proper choices of λ and $\tilde{\mu}$ are mainly determined by the noise level, the multipath delay profile and the assigned RB number for a given UE. Considering the balance between channel estimation accuracy and implementation complexity, we only set two discrete levels for λ and $\tilde{\mu}$ in our study, which can provide good enough performance with low implementation complexity (preferred in engineering practice), as shown in Section IV.

Another point should be emphasized is the operation of frequency domain windowing/dewindowing (see the dashed-line blocks in Fig. 4). Due to the frequency domain Gibbs phenomenon caused by the discontinuities at the edge of assigned consecutive RBs for a given UE, the overall channel estimation accuracy will be degraded, especially at the edge of assigned consecutive RBs. Therefore, some frequency domain window, such as Hanning window, Hamming window, Blackman window, etc. [16], can be further added to improve the channel estimation accuracy with some additional complexity. For example, Blackman window will be adopted in our following computer simulations.

$$w(n) = 0.42 - 0.5cos(2\pi n/M) + 0.08cos(4\pi n/M) \quad (9)$$

where M is the window length and $0 \leq n \leq M$. In order not to eliminate the useful signals within the assigned RBs, the window length should be larger than the assigned bandwidth ($12 \cdot RB\#$) for the corresponding UE.

IV. Computer Simulations

To demonstrate the effectiveness of our proposals, computer simulations will be provided in this section. The simulation parameters are listed in Table I. Notice that the FFT size is larger than the usable subcarrier number because of the existence of guard band. Obviously, there are totally 50 RBs in the uplink and we consider three small RB# allocation cases with RB# $= 1, 5, 10$, respectively. Furthermore, 2 typical MIMO configurations, i.e., 2×2 and 4×4, are both simulated. In our simulations, we simply chose λ and $\tilde{\mu}$ by rule of thumb, i.e., when RB# ≤ 2, $\lambda = 1$ and $\tilde{\mu} = 0.6$; when RB# > 2, $\lambda = 0.5$ and $\tilde{\mu} = 0.2$. Furthermore, the frequency domain window length is chosen to be $M = 1.1 \cdot RB\# \cdot 12$.

First, we want to evaluate the effectiveness of DMRS design with MDB CS selection. For comparison, we also simulate the case of DMRS design with random CS selection, i.e., different transmit antennas will select different CS values for their DMRS randomly, while the same CS value is not allowed to be used by different transmit antennas simultaneously. Given the improved channel estimation based on DCIR^2 at the receiver side, we compare the block error rate (BLER) performance of different DMRS designs at the transmitter side for 2×2 and 4×4 MIMO cases in Fig. 5 and Fig. 6, respectively. It is obvious that the DMRS design with MDB CS selection can achieve much better BLER performance than that of the DMRS design with random CS selection. The smaller the RB# is, the larger the performance improvement can be observed. Furthermore, with the increasing number of transmit antennas, the effectiveness of our proposal is more apparent because the interferences among different transmit antennas become more severe with the increasing transmit antenna number and MDB can reduce this kind of interference effectively. Recall that at the same time, the DMRS design with MDB CS selection needs no/few signaling modifications to be implemented into the LTE-A MIMO uplink.

Then given the DMRS design with MDB CS selection at the transmitter side, different channel estimation algorithms will be evaluated for different RB# and MIMO configurations in Fig. 7 and Fig. 8. Somewhat surprisingly, the traditional uplink channel estimation based on CPR has very poor BLER performance for all the simulated cases (RB# $= 1, 5, 10$). Meanwhile, the improved uplink channel estimation based on DCIR^2 can effectively enhance the link reliability. The reason is that even when the assigned RB# $= 10$ for a given UE, the main lobe width of CIR energy leakage is still large ($\Delta = \frac{K}{12\cdot RB\#} \approx 9$). Therefore, the CIR energy leakage problem must be handled properly to ensure the reliable uplink MIMO transmission. Moreover, frequency domain windowing/dewindowing is also helpful to further improve the BLER performance via suppressing the frequency domain Gibbs phenomenon, especially for the smaller RB# cases.

TABLE I
Simulation Parameters

Parameters	Values
Carrier frequency	2GHz
Bandwidth	10MHz
FFT size	1024
Usable subcarrier #	600
Cyclic prefix	72
Assigned RB #	1,5,10
MIMO configuration (1 Codeword, Spatial multiplexing)	2×2 4×4
Modulation	16QAM
Channel coding	Turbo,1/2 (Interleaver 288bits)
MIMO detection	MMSE
Frequency hopping	Disabled
DMRS design	Random CS selection MDB CS selection
Uplink channel estimation (within one slot)	Conventional (CPR) Improved (DCIR^2)
Inter-slot interpolation	linear
Channel model	3GPP TR 25.996 Case 2 [17]
Mobile speed	3km/h

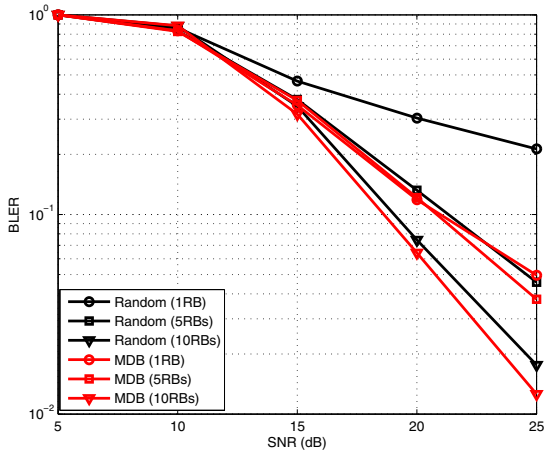

Fig. 5. BLER comparison for DMRS designs (2×2).

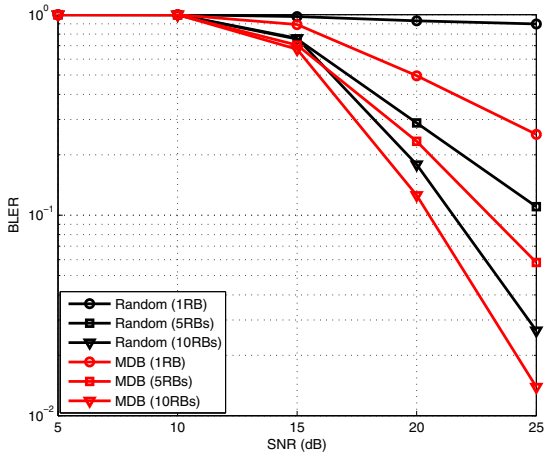

Fig. 6. BLER comparison for DMRS designs (4×4).

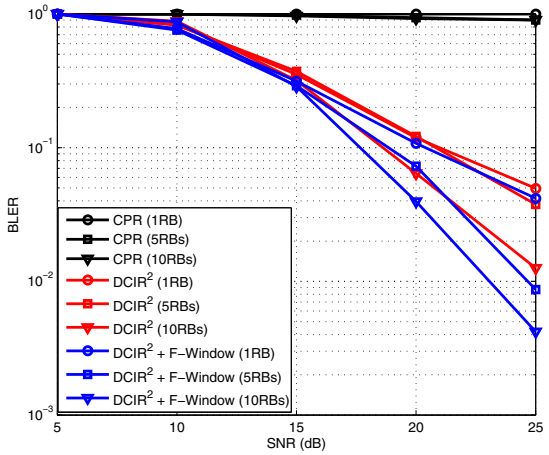

Fig. 7. BLER comparison for channel estimation (2×2).

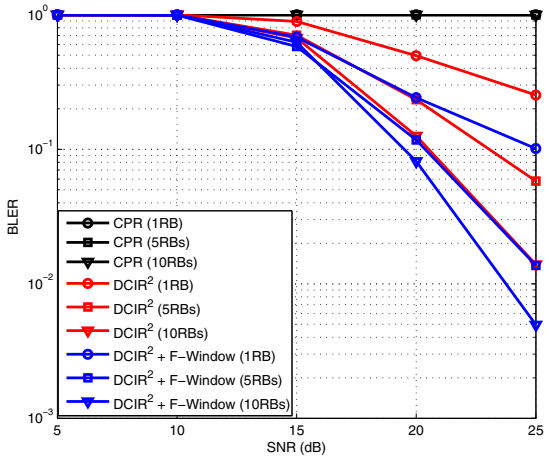

Fig. 8. BLER comparison for channel estimation (4×4).

V. Conclusion

In order to support the uplink MIMO transmission for LTE-A, we propose the backwards compatible DMRS design with MDB and the improved uplink channel estimation with DCIR^2 and frequency domain windowing/dewindowing. With no/few modifications to the current LTE specifications, the channel estimation accuracy and uplink reliability can be effectively guaranteed. Therefore, the proposal in this study is a promising solution for the DMRS design in LTE-A MIMO uplink.

References

[1] 3GPP TR 25.913, http://www.3gpp.org/ftp/specs/html-info/25913.htm
[2] 3GPP, R1-071245, "Approved report of 3GPP RAN WG1 #47bis," Feb. 2007.
[3] 3GPP TR 36.913, http://www.3gpp.org/ftp/specs/html-info/36913.htm
[4] 3GPP TS 36.211, http://www.3gpp.org/ftp/specs/html-info/36211.htm
[5] 3GPP, R1-081722, "Future 3GPP radio technologies for LTE-Advanced," Samsung, May 2008.
[6] 3GPP, R1-081948, "Proposals for LTE-Advanced technologies," NTT DOCOMO, May 2008.
[7] 3GPP, R1-082024, "A discussion on some technology components for LTE-Advanced," Ericsson, May 2008.
[8] 3GPP, R1-070190, "Uplink reference signal structure and allocation for E-UTRA," Panasonic and NTT DOCOMO, Jan. 15-19, 2007.
[9] 3GPP, R1-071643, "Sequence hopping and cyclic-shift value hopping for uplink reference signal in E-UTRA," NTT DOCOMO, Ericsson, etc., Mar. 26-30, 2007.
[10] 3GPP, R1-070432, "UL RS structure issues with frequency domain CDM," Qualcomm, Jan. 15-19, 2007.
[11] 3GPP, R1-071646, "RS and signaling structure considering future support of SU-MIMO in E-UTRA uplink," NTT DOCOMO, Fujitsu, etc., Mar. 26-30, 2007.
[12] 3GPP, R1-062102, "Orthogonal reference signal structure for uplink MIMO in E-UTRA," NTT DOCOMO, Mitsubishi, etc., Aug. 28-Sep. 1, 2006.
[13] 3GPP, R1-072116, "Discussion on uplink reference signal," NEC and NTT DOCOMO, May 7-11, 2007.
[14] 3GPP, R1-062642, "Uplink reference signal design in EUTRA," TI, Oct. 9-13, 2006.
[15] D. C. Chu, "Polyphase codes with good periodic correlation properties," *IEEE Trans. Info. Theory*, vol. 18, pp. 531-532, July 1972.
[16] A. V. Oppenheim, R. W. Schafer and J. R. Buck, *Discrete-Time Signal Processing, 2nd ed.* New Jersey: Prentice Hall, 1999.
[17] 3GPP, TR 25.996,http://www.3gpp.org/ftp/Specs/html-info/25996.htm